Dynamic Phasor Analysis of SSR Mitigation Schemes Based on Passive Phase Imbalance

Mahipalsinh C. Chudasama and Anil M. Kulkarni, *Member, IEEE*

***Abstract*—This paper presents the application of dynamic phasor analysis to understand the effect of passive phase imbalance schemes on the torsional modes of a turbine-generator system. These schemes have been proposed in the previous literature as subsynchronous resonance (SSR) countermeasures. Dynamic phasor analysis of the unbalanced system yields a linearized and time-invariant model which facilitates eigen-analysis. It is seen that large levels of phase imbalance can cause a significant movement in the subsynchronous network modal frequencies. Therefore, in specific cases, SSR can be avoided due to detuning of the torsional and network modes. However, the analysis also shows that damping torque in a series compensated network is negative at subsynchronous frequencies even with phase imbalance. Therefore, phase imbalance cannot be a general countermeasure to the problem of SSR.**

***Index Terms*—Dynamic phasors, eigen-analysis, phase imbalance, subsynchronous resonance (SSR) mitigation.**

I. Introduction

SERIES compensation is an economical and effective technique to enhance the power transfer capability of transmission lines [1]. A major concern with fixed series compensation is the possibility of adverse dynamic interaction between the network and turbine-generator shaft, resulting in growing torsional oscillations, which may damage the shaft. This phenomena is also known as subsynchronous resonance (SSR) [2]–[4]. Therefore while planning for fixed series compensation, the possibility of SSR must be analyzed. Appropriate countermeasures must be taken if this analysis reveals a potential SSR problem.

Several techniques for mitigation of SSR have been proposed in the past [2]–[4]. Edris [5] suggested two schemes of passive phase imbalance for the mitigation of SSR. Fig. 1 shows the series resonance scheme. The parallel resonance scheme is shown in Fig. 2. Imbalance is created by inserting additional capacitors and inductors in the circuit in such a manner that the system is balanced at the nominal frequency (ω_s), whereas it is unbalanced at other frequencies. C_a & C_c are additional capacitances inserted in the phases "a" and "c", respectively. The ratios C/C_a and C/C_c are used as measures of imbalance where as "C" is the capacitance per phase of the system without any imbalance. The effectiveness of the schemes for SSR mitigation have been demonstrated in specific case studies

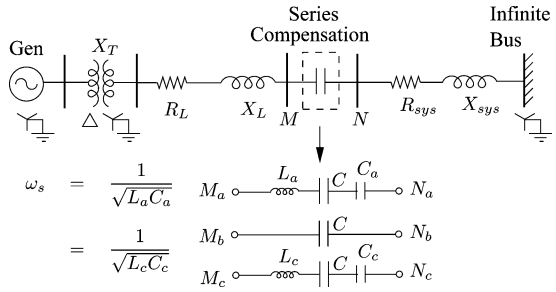

Fig. 1. Series resonance scheme.

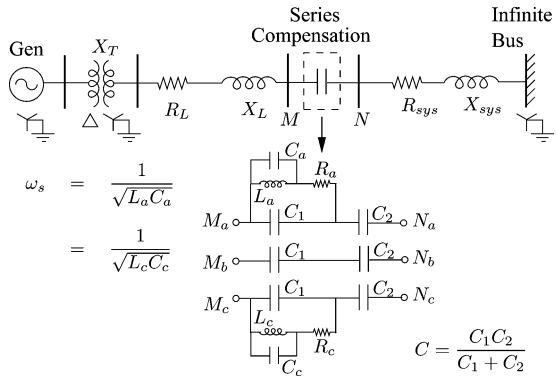

Fig. 2. Parallel resonance scheme.

by using time-domain simulations [5]. An intuitive explanation which has been put forth is that phase imbalance "reduces the energy exchange by weakening the electromagnetic coupling" [5]–[7]. However, in the absence of rigorous analysis, there is little insight into the actual mechanism of damping, or the effect of various parameters. Therefore, there have been doubts about the utility of phase imbalance as a countermeasure to SSR, in a general sense (see the discussion by Bowler in [6]). The main analytical difficulty so far has been in the modeling of phase imbalance. Conventional modeling in the "dqo" variables, using a time-variant transformation of three-phase variables, is not suitable as it yields time variant equations which do not lend themselves easily to analysis. A heuristic approach was used in [7], to extend eigen-analysis to the time variant model with dqo variables.

The dynamic phasor modeling technique has been proposed in the literature [8], [9] as an alternative to the time variant transformation of the three-phase variables to dqo variables. Dynamic phasor-based models are well suited for the analysis of unbalanced three-phase systems as well as circuits involving periodically switched devices like thyristors [10], [11]. In particular, for unbalanced systems, the dynamic phasor model is

Manuscript received June 11, 2010; revised July 19, 2010; accepted August 23, 2010. Date of publication September 23, 2010; date of current version July 22, 2011. Paper no. TPWRS-00466-2010.

The authors are with the Department of Electrical Engineering, Indian Institute of Technology Bombay, Powai, Mumbai-400076, India (e-mail: mahipal75@iitb.ac.in).

Digital Object Identifier 10.1109/TPWRS.2010.2072793

time-invariant, which makes it suitable for understanding the effect of phase imbalance on SSR.

Therefore, the main aim of this paper is to develop a linearized dynamic phasor model suitable for analysis of SSR under phase imbalance conditions. We then apply eigen-analysis tools to understand the effect of imbalance on network modal frequencies and the damping torque. It is shown that damping torque in series compensated networks is negative at subsynchronous frequencies even with phase imbalance. However, large levels of phase imbalance cause a significant movement of the network modal frequencies. Therefore in specific cases, SSR is avoided due to detuning between the torsional and network modes. These facts are illustrated using eigen-analysis and time-domain simulations using IEEE benchmark models.

The paper is organized as follows. The definition and basic relations for dynamic phasors are given in Section II. The dynamic phasor model of a synchronous machine connected to an unbalanced three-phase network is also outlined in this section. A simplified analysis is presented in Section III. Results of eigen-analysis using a detailed model, as well as time-domain simulations, are presented in Section IV.

II. Dynamic Phasor Modeling

Any periodic waveform (possibly complex) can be represented in terms of the complex Fourier coefficients as given in the following:

$$x(\tau) = \sum_{k=-\infty}^{\infty} \langle x\rangle_k(t) e^{jk\omega_s \tau} \quad \tau \in (t-T, t] \tag{1}$$

where $\omega_s = 2\pi/T$.

$\langle x\rangle_k$ represents the kth dynamic phasor of the instantaneous signal $x(t)$ and can be computed as follows:

$$\langle x\rangle_k(t) = \frac{1}{T}\int_{t-T}^{t} x(\tau) e^{-jk\omega_s\tau} d\tau. \tag{2}$$

The following important properties of dynamic phasors are used in the model derivation [8].

1) The derivative of the dynamic phasor is given by

$$\langle \dot{x}\rangle_k = \frac{d\langle x\rangle_k}{dt} = \left\langle \frac{dx}{dt}\right\rangle_k - jk\omega_s\langle x\rangle_k. \tag{3}$$

2) The dynamic phasor of the product of two signals $u(t)$ and $v(t)$ can be obtained by the discrete convolution of the corresponding dynamic phasors as follows:

$$\langle uv\rangle_k = \sum_{l=-\infty}^{\infty} \langle u\rangle_{k-l}\langle v\rangle_l. \tag{4}$$

3) Following are also used for model simplification:

$$\langle x\rangle_k = \langle x\rangle^*_{-k} \text{ When } x(t) \text{ is real} \tag{5}$$

$$\text{and } \langle x\rangle_k = \langle y\rangle^*_{-k} \text{ When, } x(t) = y(t)^* \tag{6}$$

where "*" represents the complex conjugate. Note that if $x(t)$ is periodic with a period T, then the dynamic phasor $\langle x\rangle_k(t)$ is a constant.

A. Synchronous Machine Model

The dynamic phasor model of a synchronous machine can be expressed as follows (see the outline of the derivation and the definition of variables in Appendix A):

$$\langle \dot{\psi}_{pnz}\rangle_k = -[R_s]\langle i_{pnz}\rangle_k - \langle v_{pnz}\rangle_k - jk\omega_s\langle \psi_{pnz}\rangle_k \tag{7}$$

$$\langle \dot{\psi}_r\rangle_k = -[R_r]\langle i_r\rangle_k - \langle v_r\rangle_k - jk\omega_s\langle \psi_r\rangle_k. \tag{8}$$

The algebraic equation relating the currents and fluxes is given by

$$\langle\psi\rangle_k = \langle Li\rangle_k = \langle L\rangle_{-2}\langle i\rangle_{k+2} + \langle L\rangle_{-1}\langle i\rangle_{k+1} + \langle L\rangle_0\langle i\rangle_k + \langle L\rangle_1\langle i\rangle_{k-1} + \langle L\rangle_2\langle i\rangle_{k-2}. \tag{9}$$

The mechanical equations for the mth rotor mass of the turbine-generator are given by

$$\langle \dot{\delta}_m\rangle_k = \langle \omega_m - \omega_s\rangle_k - jk\omega_s\langle\delta_m\rangle_k \tag{10}$$

$$\langle \dot{\omega}_m\rangle_k = \frac{1}{J_m}\left\{\begin{array}{l} \langle T_{mm}\rangle_k - \langle T_{em}\rangle_k - D_m\langle\omega_m\rangle_k \\ -K_{m,m-1}(\langle\delta_m\rangle_k - \langle\delta_{m-1}\rangle_k) \\ -K_{m,m+1}(\langle\delta_m\rangle_k - \langle\delta_{m+1}\rangle_k)\end{array}\right\} - jk\omega_s\langle\omega_m\rangle_k. \tag{11}$$

In what follows, the speed, angle, and electromagnetic torque corresponding to the generator rotor mass are denoted without any subscript (i.e., δ, ω, T_e).

Electromagnetic torque T_{em} is zero for all rotor masses except that of the generator. This is given by

$$\langle T_e\rangle_k = \sum_{l=-\infty}^{\infty}\langle\psi_D\rangle_{k-l}\langle i_Q\rangle_l - \sum_{l=-\infty}^{\infty}\langle\psi_Q\rangle_{k-l}\langle i_D\rangle_l \tag{12}$$

where the "$D-Q$" and "$p-n$" phasors are related as follows (see Appendix B):

$$\langle i_D\rangle_k = \frac{1}{\sqrt{2}}\left(\langle i_p\rangle_{k+1} + \langle i_n\rangle_{k-1}\right)$$

$$\langle i_Q\rangle_k = \frac{j}{\sqrt{2}}\left(\langle i_p\rangle_{k+1} - \langle i_n\rangle_{k-1}\right).$$

Similar equations are obtained for the fluxes ψ_D and ψ_Q.

Remarks:

1) The dynamic phasor model is *time-invariant* but is nonlinear due to (9) and (12). Note that the $\langle L\rangle$ matrices given in (9) are functions of $e^{j\langle\delta\rangle_0}$ (see Appendix A).
2) The equations are complex; they can be separated into real and imaginary parts and linearized around an operating point for eigen-analysis.
3) There is coupling between dynamic phasors with different k due to (9) and (12). As a result, the size of the state space is large since the equations corresponding to all k have to be represented. However, if the transients of interest have a limited bandwidth (e.g., "subsynchronous torsional and network oscillations"), then one may, as an approximation, consider only the dynamic phasors corresponding to a limited set of k.
4) The equations of a synchronous machine with balanced parameters show no coupling between the p, n, and z variables. However, when these equations are interfaced with

an external unbalanced network, such a coupling arises in the overall equations.

5) The dynamic phasor equations need to be converted to per unit form by use of appropriate base values. The parameters required for the model (per-unit resistances and inductances) can be back-calculated from the standard parameters. To avoid notational clutter, these steps are not described in this paper.

B. Dynamic Phasor Model of a Network

The derivation of a dynamic phasor model of a three-phase network is done in a similar manner; the basic network equations in "abc" variables are transformed to sequence variables and then converted to dynamic phasor form. The general form of the network equations is

$$\langle \dot{x_{pnz}} \rangle_k = A_N \langle x_{pnz} \rangle_k + B_N \langle E_{pnz} \rangle_k - jk\omega_s \langle x_{pnz} \rangle_k \quad (13)$$

$$\langle i_{pnz} \rangle_k = C_N \langle x_{pnz} \rangle_k + D_N \langle E_{pnz} \rangle_k \quad (14)$$

where $\langle x_{pnz} \rangle_k$ are the states of the network, $\langle i_{pnz} \rangle_k$ are the currents at the network port(s), and $\langle E_{pnz} \rangle_k$ are the voltages at these port(s).

If network equations in abc variables are linear time-invariant, then there is no coupling between dynamic phasors corresponding to various k. However, with imbalance, there is coupling between "pnz" variables for a given k. As in steady-state unbalanced analysis, star-delta transformers affect the "z" (zero sequence) phasors and cause phase-shifts in the $p-n$ dynamic phasors.

III. Simplified Analysis

Before proceeding for a detailed numerical analysis, let us study a simple linearized model of a synchronous generator which is represented by the classical model (voltage source behind a reactance) and is connected to an infinite bus by an unbalanced series R-L-C network. The linearized torque and "internal" voltage of the generator are given by [2]

$$\Delta T_e = E' \Delta i_Q$$

$$\Delta e_Q + j\Delta e_D = \Delta\left(\frac{\omega}{\omega_B} E' \angle\delta\right) = \frac{E'}{\omega_B}\Delta\omega + jE'\Delta\delta.$$

(e_D, e_Q, i_D, i_Q) are the generator internal voltage and current components in the synchronously rotating frame of reference. $\omega E'/\omega_B$ is the magnitude of the voltage behind the generator reactance (E' is constant).

It is assumed here, for simplicity, that the generator is operating in steady state at no load, i.e., the quiescent currents of the generator (i_{D0}, i_{Q0}) and the quiescent value of δ are zero. The quiescent frequency is equal to ω_s which is also equal to the base frequency ω_B. We now have

$$\langle \Delta T_e \rangle_0 = E' \langle \Delta i_Q \rangle_0; \quad \langle \Delta\delta \rangle_0 = \frac{1}{s}\langle \Delta\omega \rangle_0$$

$$\langle \Delta e_D \rangle_0 = E' \langle \Delta\delta \rangle_0; \quad \langle \Delta e_Q \rangle_0 = \frac{E'}{\omega_B}\langle \Delta\omega \rangle_0.$$

We can rewrite this in terms of dynamic phasors of sequence components by using the relationships between the $D-Q$ and $p-n$ dynamic phasors, which are derived in Appendix B:

$$\langle e_p \rangle_{1R} = \frac{1}{\sqrt{2}}\langle e_D \rangle_0 \quad \text{and} \quad \langle e_p \rangle_{1I} = -\frac{1}{\sqrt{2}}\langle e_Q \rangle_0 \quad (15)$$

$$\langle i_p \rangle_{1R} = \frac{1}{\sqrt{2}}\langle i_D \rangle_0 \quad \text{and} \quad \langle i_p \rangle_{1I} = -\frac{1}{\sqrt{2}}\langle i_Q \rangle_0 \quad (16)$$

where the subscripts R and I denote real and imaginary components.

Note that it is adequate to consider only $k = 0$ for the mechanical variables and $k = \pm 1$ for the electrical variables, since these dynamic phasors are decoupled from those corresponding to other values of k, due to the use of the classical model.

For an R-L-C series three-phase network connecting a generator to an infinite bus, the network equations are as given in (13), where

$$\langle x_{pnz} \rangle_1 = \begin{bmatrix} \langle i_{pnz} \rangle_1 \\ \langle V_{Cpnz} \rangle_1 \end{bmatrix}$$

$$\langle E_{pnz} \rangle_1 = \langle e_{pnz} \rangle_1 - \langle e_{Bpnz} \rangle_1$$

where e_{pnz} and e_{Bpnz} are the generator internal voltages and the infinite bus voltages, respectively, and i_{pnz} and V_{Cpnz} are the inductor currents and capacitor voltages, respectively. The infinite bus voltages are balanced and have a frequency ω_s. Therefore, $\langle e_{Bpnz} \rangle_1$ is constant. Since it is a series network, the inductor currents are the same as the generator currents. For this network, the matrices in (13) and (14) are given by

$$A_N = \omega_B \begin{bmatrix} -B_L R_m & -B_L \\ X_C & \mathbf{0} \end{bmatrix}; \quad B_N = \omega_B \begin{bmatrix} B_L \\ \mathbf{0} \end{bmatrix}$$

$$C_N = \begin{bmatrix} 1 & 0 & 0 & 0 & 0 & 0 \\ 0 & 1 & 0 & 0 & 0 & 0 \\ 0 & 0 & 1 & 0 & 0 & 0 \end{bmatrix}; \quad D_N = \begin{bmatrix} 0 & 0 & 0 \\ 0 & 0 & 0 \\ 0 & 0 & 0 \end{bmatrix}$$

where

$$P = \frac{1}{\sqrt{3}} \begin{bmatrix} 1 & 1 & 1 \\ \alpha^2 & \alpha & 1 \\ \alpha & \alpha^2 & 1 \end{bmatrix} \quad (\alpha = e^{j2\pi/3})$$

$$B_L = P^{-1} \begin{bmatrix} X_{sa} & X_m & X_m \\ X_m & X_{sb} & X_m \\ X_m & X_m & X_{sc} \end{bmatrix}^{-1} P$$

$$X_C = P^{-1} \begin{bmatrix} X_{Ca} & 0 & 0 \\ 0 & X_{Cb} & 0 \\ 0 & 0 & X_{Cc} \end{bmatrix} P$$

$$R_m = \begin{bmatrix} R_p & 0 & 0 \\ 0 & R_p & 0 \\ 0 & 0 & R_z \end{bmatrix}.$$

Note that X_s and X_m are self and mutual reactances, which include the generator reactance and unbalanced lumped elements in any phase. R_p and R_z are positive sequence and zero sequence resistances and X_C is the capacitive reactance of the R-L-C series network. The following transfer function relationship can be obtained from the network equations:

$$\langle \Delta i_p \rangle_{1I}(s) = G_1(s)\langle \Delta e_p \rangle_{1R}(s) + G_2(s)\langle \Delta e_p \rangle_{1I}(s). \quad (17)$$

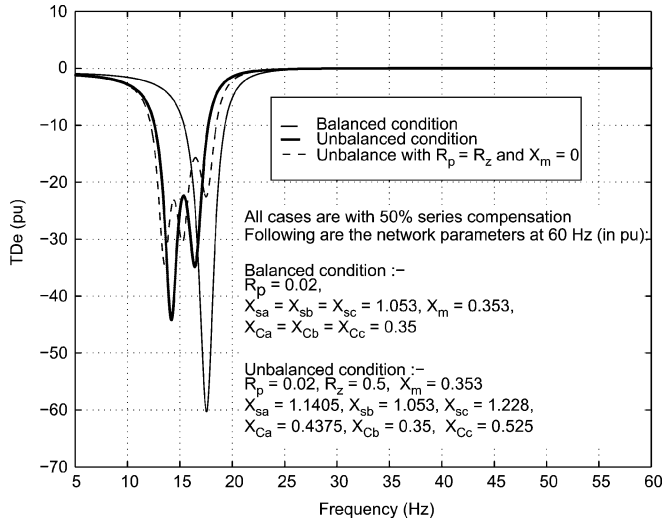

Fig. 3. Damping torque coefficient.

Using (15)–(17), we get the expression for the damping torque coefficient [2] as follows:

$$T_{De}(s) = \omega_B Re\left(\frac{\langle \Delta T_e \rangle_0(s)}{\langle \Delta\omega \rangle_0(s)}\right) = (E')^2 Re\left\{G_2(s) - \left(\frac{\omega_B}{j\omega}\right) G_1(s)\right\}. \quad (18)$$

The analytical expression for damping torque in terms of the inductances and capacitances of the network is complicated. Therefore, numerical evaluation is carried out for a specific case and is shown in Fig. 3. It is seen that T_{De} is negative at subsynchronous frequencies. This has also been verified for different network parameters, including the degree of compensation and imbalance.

To get better insight, we can get simplified expressions by assuming that $X_m = 0$ and $R_z = R_p$. Six complex pairs of eigenvalues are obtained. Note that the six complex differential equations corresponding to the network yield 12 real differential equations:

$$\lambda_1,\ \lambda_2 = a_1 \pm jb_1; \quad \lambda_3,\ \lambda_4 = a_2 \pm jb_2$$
$$\lambda_5,\ \lambda_6 = a_3 \pm jb_3; \quad \lambda_7,\ \lambda_8 = a_1 \pm jd_1$$
$$\lambda_9,\ \lambda_{10} = a_2 \pm jd_2; \quad \lambda_{11},\ \lambda_{12} = a_3 \pm jd_3$$

where

$$a_1 = -\frac{\omega_B R_p}{2X_{sa}}; \quad a_2 = -\frac{\omega_B R_p}{2X_{sb}}$$
$$a_3 = -\frac{\omega_B R_p}{2X_{sc}}$$
$$b_1, d_1 = \frac{\omega_B}{2X_{sa}}\left(2X_{sa} \mp \sqrt{4X_{sa}X_{Ca} - R_p^2}\right)$$
$$b_2, d_2 = \frac{\omega_B}{2X_{sb}}\left(2X_{sb} \mp \sqrt{4X_{sb}X_{Cb} - R_p^2}\right)$$
$$b_3, d_3 = \frac{\omega_B}{2X_{sc}}\left(2X_{sc} \mp \sqrt{4X_{sc}X_{Cc} - R_p^2}\right).$$

λ_1, λ_3, and λ_5 are the important eigenvalues which affect the damping torque at subsynchronous frequencies. The damping torque coefficient can be approximated as follows near these frequencies:

$$T_{De}(s) = \sum_{n=1}^{12} \frac{\mathcal{R}_i}{s - \lambda_i} \approx \frac{\mathcal{R}_1}{s - \lambda_1} + \frac{\mathcal{R}_3}{s - \lambda_3} + \frac{\mathcal{R}_5}{s - \lambda_5} \quad (19)$$

where $\mathcal{R}_i$ denotes the residue of the transfer function (18) and corresponding to the ith eigenvalue. The approximate expression is analytically determined to be as follows:

$$T_{De}(j\Omega) \approx \frac{(E')^2}{6R_p}\left(1 - \frac{\omega_B}{\Omega}\right)\left(\frac{1}{d_{11}} + \frac{1}{d_{22}} + \frac{1}{d_{33}}\right) - \frac{(E')^2}{6}\left(1 - \frac{\omega_B}{\Omega}\right) \times \left(\frac{\Omega - b_1}{a_1 c_1 d_{11}} + \frac{\Omega - b_2}{a_2 c_2 d_{22}} + \frac{\Omega - b_3}{a_3 c_3 d_{33}}\right) \quad (20)$$
$$\approx \frac{(E')^2}{6R_p}\left(1 - \frac{\omega_B}{\Omega}\right)\left(\frac{1}{d_{11}} + \frac{1}{d_{22}} + \frac{1}{d_{33}}\right) \quad (21)$$

where

$$d_{11} = 1 + \left(\frac{\Omega - b_1}{a_1}\right)^2$$
$$d_{22} = 1 + \left(\frac{\Omega - b_2}{a_2}\right)^2$$
$$d_{33} = 1 + \left(\frac{\Omega - b_3}{a_3}\right)^2$$

and

$$c_1 = \sqrt{4X_{sa}X_{Ca} - R_p^2}$$
$$c_2 = \sqrt{4X_{sb}X_{Cb} - R_p^2}$$
$$c_3 = \sqrt{4X_{sc}X_{Cc} - R_p^2}.$$

Note that the magnitude of the second term in (20) is much smaller than the first term if $R_p \ll X_s$ and a realistic range of compensation level ($X_C = 0.1$ to $0.7X_s$) is used. It is easily evident that the simplified expression of damping torque (21) is negative for Ω in the subsynchronous range. Therefore, it appears that one cannot cause positive damping of subsynchronous torsional modes using an unbalanced network alone.

However, it is seen that there is significant shift in the modal frequencies with the introduction of imbalance. In Fig. 3, the frequency at which damping torque is minimum shifts significantly with imbalance. Therefore, it seems possible to detune the network modes using phase imbalance (if there is a coincidence with a torsional modal frequency under balanced conditions), and thereby avoid an SSR situation. It is also seen that the critical network modal frequencies are lowered due to phase imbalance. The negative peak of the damping torque is significantly reduced as well.

IV. Eigen-Analysis With Detailed Models

We now check the validity of modeling methodology as well as evaluate the phase imbalance scheme for mitigation of SSR.

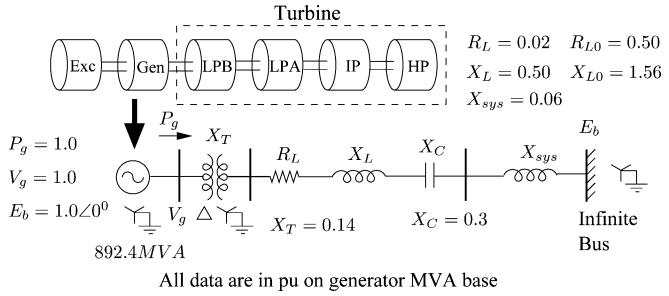

Fig. 4. IEEE First Benchmark Model (FBM).

TABLE I
TORSIONAL AND NETWORK MODES WITH FBM AND SERIES RESONANCE SCHEME

Torsional modes					
Mode	**Mode freq. (rad/s)**	**Real part of eigenvalue**			
		Balanced	**Case-I**	**Case-II**	**Case-III**
1	99.5	0.02	0.04	**0.19**	**2.26**
2	127.1	0.008	**0.15**	0.05	**0.15**
3	159.8	**0.59**	0.06	0.03	0.02
4	202.8	0.005	0.004	0.007	**0.012**
5	298.2	0	0	0	0

Network modes			
Balanced	**Case-I**	**Case-II**	**Case-III**
-3.70±j**155.64**	-3.66±j**130.33**	-3.40±j**112.34**	-4.77±j**98.09**
-4.71±j154.56	-4.14±j147.05	-4.79±j139.20	-6.40±j**126.32**
-53.58±j230.81	-50.95±j217.13	-48.19±j208.9	-44.63±j**201.59**
-53.58±j523.17	-50.94±j536.85	-48.18±j545.09	-44.61±j552.40
-4.69±j598.82	-4.10±j606.88	-4.73±j614.56	-6.20±j627.33
-3.09±j599.39	-3.44±j623.21	-3.20±j640.84	-2.56±j656.26
Case-I : $C/C_a = 0.25,\ C/C_c = 0.5$			
Case-II : $C/C_a = 0.5,\ C/C_c = 1.0$			
Case-III : $C/C_a = 1.0,\ C/C_c = 1.5$			

The systems are adapted from IEEE First and Second Benchmark Models (FBM and SBM). Both series and parallel schemes are considered (see Figs. 1 and 2).

For the eigen-analysis, we consider a model in which the dynamic phasors corresponding to $k = \pm 1$ for the stator "pnz" variables, $k = 0, 2$ for the rotor variables and $k = 0$ for the mechanical variables, are represented, and the others are neglected (see the remarks in Section II-A). Note that the network and torsional transients of interest lie in the subsynchronous range, for which this seems to be a reasonable choice. As we shall see, this gives results which match well with the detailed simulations carried out using the abc variables.

A. IEEE First Benchmark System

The IEEE FBM is shown in Fig. 4 for which the data are taken from [12]. Mechanical (viscous) damping is not considered for this test system. The compensation level at the nominal frequency is 43%. The system has five torsional modes, out of which four are unstable (since mechanical damping is not considered, the results are pessimistic) for the balanced case. The fifth mode is not affected by the electrical network [2].

Table I shows the variation in real parts of the torsional modes with series scheme for different cases of imbalance. The torsional modal frequencies are determined mainly by the mechanical stiffness and mass, and are practically unaffected by the electrical network. The degree of imbalance is quantified by the ratios C/C_a and C/C_c. These values are chosen near-about the values used in Edris's paper [5].

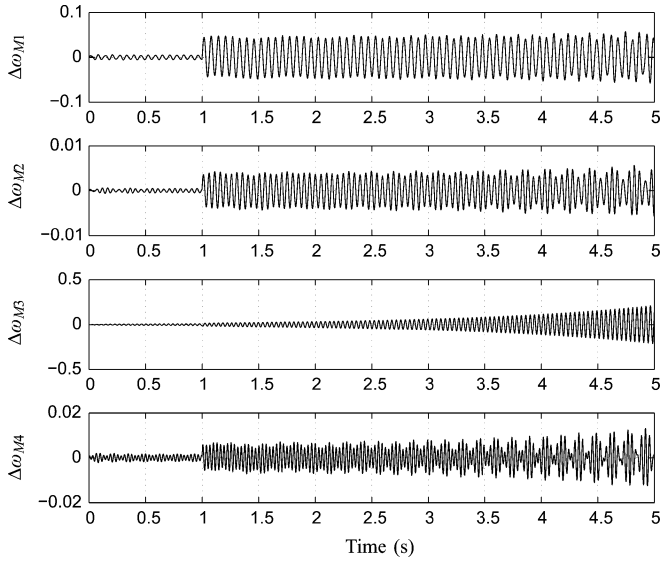

Fig. 5. Modal speed deviations (rad/s) without imbalance for FBM.

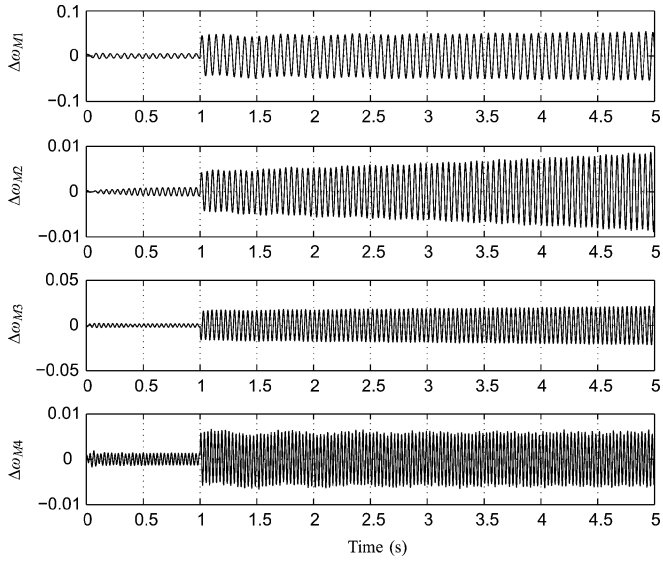

Fig. 6. Modal speed deviations (rad/s) with series resonance scheme and $C/C_a = 0.25$, $C/C_c = 0.5$ for FBM.

It can be observed that while the critical network modal frequencies change and get detuned from one or the other torsional mode, it is difficult to ensure detuning of all torsional modes simultaneously. Hence, the system is unstable for all the cases which are considered, in spite of phase imbalance.

In order to verify the results, detailed three-phase time-domain simulation is done using Matlab/Simulink [14]. To excite the torsional modes, mechanical torque of all turbines is changed from 100% to 95% at $t = 1$ s. We have plotted the modal speed deviations corresponding to the first four torsional modes, for the balanced case and case-I, in Figs. 5 and 6, respectively.

TABLE II
TORSIONAL AND NETWORK MODES WITH FBM AND PARALLEL RESONANCE SCHEME

Torsional modes					
Mode	Mode freq. (rad/s)	Real part of eigenvalue			
		Balanced	Case-I	Case-II	Case-III
1	99.5	0.02	0.02	**0.18**	0.04
2	127.1	0.008	0.04	0.03	0.06
3	159.8	**0.59**	0.08	0.08	0.05
4	202.8	0.005	**0.10**	**0.19**	**0.24**
5	298.2	0	0	0	0

Network modes			
Balanced	**Case-I**	**Case-II**	**Case-III**
-4.71$\pm j$**154.56**	-3.03$\pm j$134.04	-2.67$\pm j$**106.52**	-2.52$\pm j$120.84
-3.70$\pm j$155.64	-3.79$\pm j$149.14	-3.63$\pm j$136.95	-3.85$\pm j$135.31
-53.58$\pm j$230.81	-47.20$\pm j$234.28	-53.98$\pm j$238.11	-53.54$\pm j$238.48
0.0 $\pm j$376.99	-11.18$\pm j$**198.45**	-7.23$\pm j$174.23	-8.40$\pm j$178.09
0.0 $\pm j$376.99	-5.90$\pm j$240.97	-4.70$\pm j$**207.87**	-3.75$\pm j$**206.88**
0.0 $\pm j$376.99	-5.89$\pm j$512.99	-4.53$\pm j$545.90	-3.54$\pm j$546.82
0.0 $\pm j$376.99	-11.08$\pm j$555.50	-7.14$\pm j$579.61	-8.32$\pm j$575.81
-53.58$\pm j$523.17	-47.20$\pm j$519.70	-53.98$\pm j$515.87	-53.54$\pm j$515.50
-3.09$\pm j$599.39	-3.73$\pm j$604.85	-3.58$\pm j$616.86	-3.81$\pm j$618.49
-4.69$\pm j$598.82	-2.95$\pm j$619.70	-2.50$\pm j$646.96	-2.45$\pm j$632.94
Case-I : $C/C_a = 0.5,\ C/C_c = 1.0$			
Case-II : $C/C_a = 0.25,\ C/C_c = 0.5$			
Case-III : $C/C_a = 0.35,\ C/C_c = 0.45$			

Note that the modal speed deviation $\Delta\omega_{Ml}$ corresponding to a torsional mode "l" is approximately obtained as follows:

$$\Delta\omega_{Ml} = q_l^T \left[\Delta\omega_{HP} \quad \cdots \quad \Delta\omega_{Exc}\right]^T$$

where q_l^T is a vector containing the left eigenvector components corresponding to individual angular speed deviations of the rotor masses of the turbine-generator system ($\Delta\omega_{HP} \quad \cdots \quad \Delta\omega_{Exc}$). Modal speed deviations are shown in order to view the effect on individual modes separately.

From Fig. 5, it is clear that with the balanced condition, un-damping of the modal speed deviation for mode-3 is highest as it is tuned to one of the network modes. In case-I, mode-3 gets detuned but mode-2 is tuned to one of the network modes. Hence, $\Delta\omega_{M2}$ shows an unstable response as shown in Fig. 6, which is as predicted by the eigen-analysis.

In case of parallel resonance scheme, the capacitive reactance which is shunted by a parallel branch is taken as 20% of total X_c per phase and $R_a = R_c = 1\,\Omega$. Table II shows real parts of torsional modes with parallel resonance scheme. The difference here is that reduction in C/C_a ratio implies increased degree of imbalance. The results and conclusions are similar to those obtained with the series resonance scheme: all modes cannot be detuned simultaneously, and hence, the system is unstable even with imbalance. The results with the parallel resonance scheme are also verified with time-domain simulations, although they are not shown here.

B. IEEE Second Benchmark System

The IEEE Second Benchmark Model [13] is taken as another test system—see Fig. 7. Mechanical damping has been considered, unlike in the previous test cases. The rotor of the synchronous machine is modeled with four lumped masses. Out of

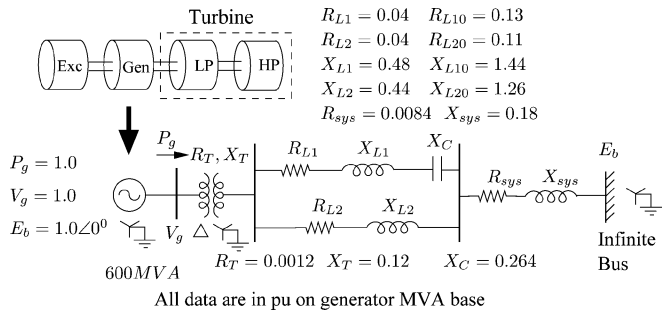

Fig. 7. IEEE Second Benchmark Model (SBM).

TABLE III
TORSIONAL AND NETWORK MODES WITH SBM AND SERIES RESONANCE SCHEME

Torsional modes					
Mode	Mode freq. (rad/s)	Real part of eigenvalue			
		Balanced	Case-I	Case-II	Case-III
1	155.1	**0.37**	**0.13**	**0.04**	**-0.005**
2	203.5	-0.04	-0.05	-0.05	-0.04
3	321.1	-0.05	-0.05	-0.05	-0.05

Network modes			
Balanced	**Case-I**	**Case-II**	**Case-III**
-15.64$\pm j$148.03	-13.30$\pm j$123.94	-11.65$\pm j$106.48	-10.19$\pm j$91.44
-15.44$\pm j$**148.21**	-14.77$\pm j$**140.23**	-13.96$\pm j$**132.23**	-12.63$\pm j$**119.14**
-16.54$\pm j$224.64	-16.09$\pm j$212.65	-15.91$\pm j$205.68	-15.82$\pm j$199.56
-16.54$\pm j$529.34	-16.09$\pm j$541.33	-15.91$\pm j$548.30	-15.81$\pm j$554.42
-15.63$\pm j$605.94	-14.62$\pm j$613.88	-13.87$\pm j$621.86	-12.58$\pm j$634.90
-14.98$\pm j$605.98	-13.23$\pm j$630.12	-11.61$\pm j$647.54	-10.15$\pm j$662.54
Case-I : $C/C_a = 0.25,\ C/C_c = 0.5$			
Case-II : $C/C_a = 0.5,\ C/C_c = 1.0$			
Case-III : $C/C_a = 1.0,\ C/C_c = 1.5$			

three torsional modes, one is unstable. The torsional Mode-3 is not affected much by the electrical network.

The variation of the real parts of the eigenvalues corresponding to the torsional modes is shown in Table III. The results show that the damping of the first torsional mode improves due to imbalance. A comparison of the network and torsional modes shows that the network modal frequency reduces with increased imbalance. The difference in frequencies between the critical network mode and the lowest frequency torsional mode increases, thereby reducing the adverse effect of the electrical network on this torsional mode. Eventually for Case-III, the torsional modes become stable.

Although not shown in Table III, if the mechanical damping is neglected, then the real part of the eigenvalue corresponding to 155.1 rad/s torsional mode is found to change from $+0.42$ (balanced case) to $+0.05$ (Case-III). Moreover, torsional modes 2 and 3 are found to have small positive real parts for all the cases. This shows that the phase imbalance scheme does not cause positive damping. However in this system, the de-stabilizing effect of the network can be reduced (due to detuning) to a point at which the mechanical (viscous) damping is adequate to ensure stability of the torsional modes.

Table IV shows the real parts of eigenvalues corresponding to different torsional modes with the parallel resonance scheme. It is found that the system is stable for Case-II but it is unstable for both smaller as well as larger imbalance. This is because of the near-coincidence of third network mode with the lowest frequency torsional mode (Case-III). Time-domain simulation results are shown in Figs. 8 and 9. The disturbance considered

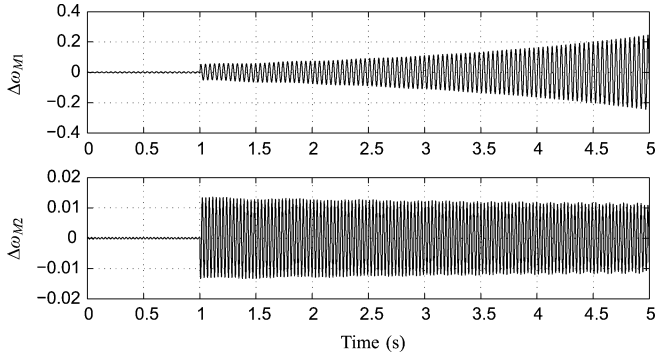

Fig. 8. Modal speed deviations (rad/s) without imbalance for SBM.

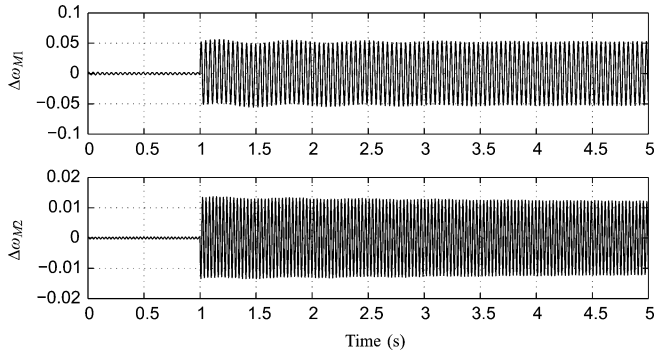

Fig. 9. Modal speed deviations (rad/s) with parallel resonance scheme and $C/C_a = 0.35, C/C_c = 0.45$ for SBM.

TABLE IV
TORSIONAL AND NETWORK MODES WITH SBM AND PARALLEL RESONANCE SCHEME

Torsional modes					
Mode	Mode freq. (rad/s)	Real part of eigenvalue			
		Balanced	Case-I	Case-II	Case-III
1	155.1	**0.37**	**0.12**	**-0.004**	**0.17**
2	203.5	-0.04	-0.04	-0.03	-0.04
3	321.1	-0.05	-0.05	-0.05	-0.05

Network modes			
Balanced	**Case-I**	**Case-II**	**Case-III**
-15.64±j148.03	-10.40±j130.07	-7.92±j117.98	-3.57±j80.15
-15.44±j**148.21**	-13.95±j**143.21**	-9.46±j132.04	-5.21±j106.54
-16.54±j224.64	-8.65±j188.62	-10.32±j**171.21**	-14.42±j**159.93**
0.0 ±j376.99	-8.64±j229.89	-8.74±j203.95	-12.71±j186.44
0.0 ±j376.99	-8.71±j252.89	-14.72±j242.43	-15.99±j239.20
0.0 ±j376.99	-8.71±j501.09	-14.72±j511.55	-15.99±j514.78
0.0 ±j376.99	-8.64±j524.08	-8.72±j549.99	-12.67±j567.48
-16.54±j529.34	-8.65±j565.34	-10.29±j582.69	-14.21±j593.98
-15.63±j605.94	-13.79±j610.90	-9.43±j622.03	-5.21±j647.46
-14.98±j605.98	-10.35±j624.00	-7.91±j636.05	-3.56±j673.82

Case-I : $C/C_a = 0.5,\ C/C_c = 1.0$
Case-II : $C/C_a = 0.35,\ C/C_c = 0.45$
Case-III : $C/C_a = 0.15,\ C/C_c = 0.25$

is a 5% change in mechanical torque, as before. The simulations support the inferences obtained from eigen-analysis.

To summarize: it is observed from the detailed study of two test cases and the derivation in Section III that phase imbalance does not cause positive damping by itself, but reduces the negative peaks in the damping torque and leads to a change in network modal frequencies. If the torsional modal frequencies are few or well-spaced, SSR can be avoided due to detuning effect. Even here, switched elements would be required to ensure that detuning persists even with changes in the network conditions. If there are several closely spaced torsional modes, then it is difficult to simultaneously detune all of them.

V. CONCLUSION

An investigation of the series and parallel passive phase imbalance schemes as countermeasures to SSR is presented in this paper. This analysis is facilitated by dynamic phasor modeling since it yields a time-invariant system of equations.

Simplified analysis indicates that the damping torque provided by a passive unbalanced network is not positive in the subsynchronous frequency range. However, the frequencies of the network subsynchronous modes change due to phase imbalance. Therefore, phase imbalance schemes can be used to prevent a torsional and network mode resonance condition if it exists for a certain level of balanced compensation. However, this is problematic if several torsional modes are present and when network conditions change.

These conclusions have been verified by detailed eigen-analysis and time-domain simulations. The results of this paper support the assessment of Bowler (in the discussion in [6]) that passive phase imbalance schemes cannot be a solution to SSR in a general sense.

APPENDIX A
SYNCHRONOUS MACHINE MODEL

The equations of a synchronous machine which relate fluxes "ψ", currents "i", and applied voltages "v" are [2]

$$\begin{aligned}
\dot{\psi}_s &= -[R_s]i_s - v_s \\
\dot{\psi}_r &= -[R_r]i_r - v_r \quad \text{and} \\
\begin{bmatrix}\psi_s \\ \psi_r\end{bmatrix} &= \begin{bmatrix}L_{ss}(\theta) & L_{sr}(\theta) \\ L_{rs}(\theta) & L_{rr}\end{bmatrix}\begin{bmatrix}i_s \\ i_r\end{bmatrix} \\
&\text{where} \\
\psi_s &= [\psi_a\ \psi_b\ \psi_c]^T, \quad \psi_r = [\psi_f\ \psi_h\ \psi_g\ \psi_k]^T \\
v_s &= [v_a\ v_b\ v_c]^T, \quad v_r = [-v_f\ 0\ 0\ 0]^T \\
i_s &= [i_a\ i_b\ i_c]^T, \quad i_r = [i_f\ i_h\ i_g\ i_k]^T \\
[R_s] &= \text{diag}[R_a\ R_a\ R_a], \\
[R_r] &= \text{diag}[R_f\ R_h\ R_g\ R_k] \\
\theta &= \omega_s t + \delta.
\end{aligned}$$

In the above equations, subscripts "a, b, c" refers to stator three-phase quantities. Subscripts "f, g, h, k" refers to field winding and damper windings parameters. "θ" is the generator electrical angular position while "δ" is the generator electrical angular position in a synchronously rotating frame (rotating at ω_s rad/s).

The R and L denote resistances and inductances of the windings. The stator abc quantities are transformed to pnz quantities using the following transformation:

$$\begin{bmatrix}f_a \\ f_b \\ f_c\end{bmatrix} = \frac{1}{\sqrt{3}}\begin{bmatrix}1 & 1 & 1 \\ \alpha^2 & \alpha & 1 \\ \alpha & \alpha^2 & 1\end{bmatrix}\begin{bmatrix}f_p \\ f_n \\ f_z\end{bmatrix} \tag{22}$$

where $\alpha = 1\angle 120^0 = e^{j2\pi/3}$ and "f" may be any of the variables ψ, i, or v. Therefore

$$\begin{aligned}\dot{\psi_{pnz}} &= -[R_s]i_{pnz} - v_{pnz}\\ \dot{\psi_r} &= -[R_r]i_r - v_r\\ \psi = Li &= \begin{bmatrix} L'_{ss}(\theta) & L'_{sr}(\theta)\\ L'_{rs}(\theta) & L_{rr}\end{bmatrix}\begin{bmatrix} i_{pnz}\\ i_r\end{bmatrix}\end{aligned}$$

where

$$\begin{aligned}\psi_{pnz} &= [\,\psi_p \quad \psi_n \quad \psi_z\,]^T;\\ v_{pnz} &= [\,v_p \quad v_n \quad v_z\,]^T;\\ i_{pnz} &= [\,i_p \quad i_n \quad i_z\,]^T;\\ \psi &= \begin{bmatrix}\psi_{pnz}\\ \psi_r\end{bmatrix};\quad i = \begin{bmatrix} i_{pnz}\\ i_r\end{bmatrix}.\end{aligned}$$

From the above equations, we obtain the dynamic phasor relationships of Section II-A. The inductance matrix L is a function of θ. In particular, it consists of terms like $e^{\pm j\theta}$ and $e^{\pm j2\theta}$. Therefore

$$\langle Li\rangle_k = \langle L\rangle_{-2}\langle i\rangle_{k+2} + \langle L\rangle_{-1}\langle i\rangle_{k+1} + \langle L\rangle_0\langle i\rangle_k + \langle L\rangle_1\langle i\rangle_{k-1} + \langle L\rangle_2\langle i\rangle_{k-2}.$$

Important: If higher frequency variations in δ are ignored, i.e., $\delta(\tau) \approx \langle\delta\rangle_0(t)$ for $\tau \in (t-T, t]$, then $\langle Li\rangle_k$ are a function of $e^{j\langle\delta\rangle_0}$ but independent of θ.

The mechanical equations for a rotor mass "m" of a turbine-generator system, connected by an elastic shaft to masses $m-1$ and $m+1$ are given by

$$\begin{aligned}\dot{\delta_m} &= \omega_m - \omega_s\\ \dot{\omega_m} &= \frac{1}{J_m}\left\{\begin{array}{c} T_{mm} - T_e - D_m\,\omega_m\\ -K_{m,m-1}(\delta_m - \delta_{m-1})\\ -K_{m,m+1}(\delta_m - \delta_{m+1})\end{array}\right\}.\end{aligned}$$

For notational simplicity, a 2-pole machine is assumed, where

J_m	inertia of the rotor mass "m";
D_m	mechanical damping coefficient of mass "m";
$K_{i,j}$	shaft stiffness coefficient for section $i-j$;
T_{mm}	mechanical torque acting on mass "m";
T_e	electrical torque (present only for the generator);
δ_m	angular position of mass "m" in a synchronously rotating frame;
ω_m	angular speed of rotor mass "m".

We get (10) and (11) using the above set of equations.

Note that the electromagnetic torque of the generator can be expressed in the $d-q$ variables (obtained from Parks transformation of the instantaneous three-phase variables) or $D-Q$ variables (synchronous transformation) as follows [2]:

$$\begin{aligned}T_e &= \psi_d i_q - \psi_q i_d = \psi_D i_Q - \psi_Q i_D\\ \therefore \langle T_e\rangle_k &= \sum_{l=-\infty}^{\infty}\langle\psi_D\rangle_{k-l}\langle i_Q\rangle_l - \sum_{l=-\infty}^{\infty}\langle\psi_Q\rangle_{k-l}\langle i_D\rangle_l.\end{aligned}$$

Using the relationships derived in Appendix B, we obtain

$$\begin{aligned}\langle f_D\rangle_k &= \frac{1}{\sqrt{2}}\left(\langle f_p\rangle_{k+1} + \langle f_n\rangle_{k-1}\right)\\ \langle f_Q\rangle_k &= \frac{j}{\sqrt{2}}\left(\langle f_p\rangle_{k+1} - \langle f_n\rangle_{k-1}\right).\end{aligned}$$

Thus, the electrical torque can be expressed in terms of the $p-n$ dynamic phasors.

APPENDIX B
RELATION BETWEEN $DQ0$ AND pnz VARIABLES

Use the transformation in synchronously rotating reference frame given in the equation at the bottom of the page.

Similarly

$$\begin{aligned}f_Q &= \frac{1}{j\sqrt{2}}\left(e^{j\omega_s t}f_n - e^{-j\omega_s t}f_p\right) \quad \& \quad f_0 = f_z\\ \therefore\ f_p e^{-j\omega_s t} &= \frac{1}{\sqrt{2}}(f_D - jf_Q) \text{ and}\\ f_n e^{j\omega_s t} &= \frac{1}{\sqrt{2}}(f_D + jf_Q).\end{aligned}$$

In terms of dynamic phasors, the above equations are

$$\begin{aligned}\langle f_p\rangle_{k+1} &= \frac{1}{\sqrt{2}}(\langle f_D\rangle_k - j\langle f_Q\rangle_k)\\ \langle f_n\rangle_{k-1} &= \frac{1}{\sqrt{2}}(\langle f_D\rangle_k + j\langle f_Q\rangle_k).\end{aligned}$$

$$\begin{aligned}\begin{bmatrix} f_D\\ f_Q\\ f_0\end{bmatrix} &= \sqrt{\frac{2}{3}}\begin{bmatrix}\cos\omega_s t & \cos\left(\omega_s t - \frac{2\pi}{3}\right) & \cos\left(\omega_s t + \frac{2\pi}{3}\right)\\ \sin\omega_s t & \sin\left(\omega_s t - \frac{2\pi}{3}\right) & \sin\left(\omega_s t + \frac{2\pi}{3}\right)\\ \frac{1}{\sqrt{2}} & \frac{1}{\sqrt{2}} & \frac{1}{\sqrt{2}}\end{bmatrix}\begin{bmatrix} f_a\\ f_b\\ f_c\end{bmatrix}\\ \therefore f_D &= \frac{1}{\sqrt{6}}\begin{bmatrix}\{e^{j\omega_s t} + e^{-j\omega_s t}\}f_a\\ +\{e^{j(\omega_s t - 2\pi/3)} + e^{-j(\omega_s t - 2\pi/3)}\}f_b\\ +\{e^{j(\omega_s t + 2\pi/3)} + e^{-j(\omega_s t + 2\pi/3)}\}f_c\end{bmatrix}\\ &= \frac{1}{\sqrt{2}}(e^{j\omega_s t}f_n + e^{-j\omega_s t}f_p)\end{aligned}$$

REFERENCES

[1] K. R. Padiyar, *FACTS Controllers in Power Transmission and Distribution*. New Delhi, India: New Age Int., 2009.

[2] K. R. Padiyar, *Analysis of Subsynchronous Resonance in Power Systems*. Norwell, MA: Kluwer, 1999.

[3] P. Kundur, *Power System Stability and Control*. New York: McGraw-Hill, 1996.

[4] P. M. Anderson, J. E. Van Ness, and B. L. Agrawal, *Subsynchronous Resonance in Power Systems*. New York: Wiley, 1990.

[5] A.-A. Edris, "Series compensation schemes reducing the potential of subsynchronous resonance," *IEEE Trans. Power Syst.*, vol. 5, no. 1, pp. 219–226, Feb. 1990.

[6] A.-A. Edris, "Subsynchronous resonance countermeasure using phase imbalance," *IEEE Trans. Power Syst.*, vol. 8, no. 4, pp. 1438–1447, Nov. 1993.

[7] M. R. Iravani and A.-A. Edris, "Eigen-analysis of series compensation schemes reducing the potential of subsynchronous resonance," *IEEE Trans. Power Syst.*, vol. 10, no. 2, pp. 876–883, May 1995.

[8] A. M. Stankovic and T. Aydin, "Analysis of asymmetrical faults in power systems using dynamic phasors," *IEEE Trans. Power Syst.*, vol. 15, no. 3, pp. 1062–1068, Aug. 2000.

[9] A. M. Stankovic, S. R. Sanders, and T. Aydin, "Dynamic phasors in modeling and analysis of unbalanced polyphase AC machines," *IEEE Trans. Energy Convers.*, vol. 17, no. 1, pp. 107–113, Mar. 2002.

[10] A. M. Stankovic, P. Mattavelli, V. Caliskan, and G. C. Verghese, "Modeling and analysis of FACTS devices with dynamic phasors," in *Proc. IEEE Power Eng. Soc. Winter Meeting*, Jan. 2000, vol. 2, pp. 1440–1446.

[11] P. Mattavelli, A. M. Stankovic, and G. C. Verghese, "SSR analysis with dynamic phasor model of thyristor-controlled series capacitor," *IEEE Trans. Power Syst.*, vol. 14, no. 1, pp. 200–208, Feb. 1999.

[12] IEEE Subsynchronous Resonance Task Force, "First benchmark model for computer simulation of subsynchronous resonance," *IEEE Trans. Power App. Syst.*, vol. PAS-96, no. 5, pp. 1565–1572, Sep. 1977.

[13] IEEE Subsynchronous Resonance Task Force, "Second benchmark model for computer simulation of subsynchronous resonance," *IEEE Trans. Power App. Syst.*, vol. PAS-104, no. 5, pp. 1057–1066, May 1985.

[14] MATLAB and SIMULINK Demos and Documentation. [Online]. Available: http://www.mathworks.com/access/helpdesk/help/techdoc/.

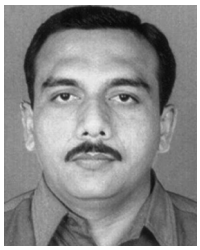

Mahipalsinh C. Chudasama received the B.E. degree in electrical engineering from the North Gujarat University, Patan, India, in 1996 and the M.E. degree in electrical engineering from the Gujarat University, Ahmedabad, India, in 2005. He is pursuing the Ph.D. degree at the Indian Institute of Technology, Bombay, India.

Currently, he is an Assistant Professor at S. S. Engineering College, Bhavnagar, India. His current research interests are power system dynamics and modeling of machines.

Anil M. Kulkarni (M'07) received the B.E. degree in electrical engineering from the University of Roorkee, Roorkee, India, in 1992, and the M.E. degree in electrical engineering and Ph.D. degree from the Indian Institute of Science, Bangalore, India, in 1994 and 1998, respectively.

He is currently an Associate Professor at the Indian Institute of Technology, Bombay, India. His research interests include power system dynamics and FACTS.